The Journal of Immunology
RESEARCH ARTICLE | AUGUST 15 2017

Virus-Triggered ATP Release Limits Viral Replication through Facilitating IFN-β Production in a P2X7-Dependent Manner FREE

Chengfei Zhang; ... et. al

J Immunol (2017) 199 (4): 1372–1381.
https://doi.org/10.4049/jimmunol.1700187

Virus-Triggered ATP Release Limits Viral Replication through Facilitating IFN-β Production in a P2X7-Dependent Manner

Chengfei Zhang,* Hongwang He,* Li Wang,* Na Zhang,* Hongjun Huang,* Qingqing Xiong,* Yan Yan,* Nannan Wu,* Hua Ren,* Honghui Han,† Mingyao Liu,* Min Qian,* and Bing Du*

Accumulating evidence shows that innate immune responses are associated with extracellular nucleotides, particularly ATP. In this article, we demonstrate extensive protection of ATP/P2X7 signaling in a host against viral infection. Interestingly, we observed a significant increase in ATP as a danger signal in vesicular stomatitis virus (VSV)-infected cell supernatant and VSV-infected mice in an exocytosis- and pannexin channel–dependent manner. Furthermore, extracellular ATP reduces the replication of VSV, Newcastle disease virus, murine leukemia virus, and HSV in vivo and in vitro through the P2X7 receptor. Meanwhile, ATP significantly increases IFN-β expression in a concentration- and time-dependent manner. Mechanistically, ATP facilitates IFN-β secretion through P38/JNK/ATF-2 signaling pathways, which are crucial in promoting antiviral immunity. Taken together, these results demonstrate the protective role of extracellular ATP and P2X7 in viral infection and suggest a potential therapeutic role for ATP/P2X7 in viral diseases. ***The Journal of Immunology*****, 2017, 199: 1372–1381.**

As the basic elements of all living organisms, nucleosides and nucleotides perform a multiplicity of functions as the building blocks of nucleic acids, coenzymes, allosteric modulators, energy intermediates, and intracellular and extracellular messengers. Since the "Danger" hypothesis was proposed in 1994 (1), many danger-associated molecular patterns, such as nuclear or cytosolic proteins, have been shown to be involved in the regulation of innate immune responses (2). Among them, the nucleotides ATP, UTP, and UDP that are released into the extracellular space can also serve as danger signals by activating purinergic receptors (3). Not only is ATP the universal energy currency, it also plays a completely different role in the extracellular compartment as a signaling molecule, where it activates purinergic P2 receptors (4). Based on their structure and distinct signal-transduction mechanisms, P2 receptors can be subdivided into metabotropic P2Y receptors (P2YRs), which are G protein coupled, and ionotropic P2X receptors (P2XRs), which are nucleotide-gated ion channels (5). Interestingly, ATP can activate all P2XRs and particular P2YRs, including $P2RY_2$ and $P2RY_{11}$, which are important in regulating immune responses (6, 7). Our previous study showed that TLR-triggered ATP release protects mice against bacterial infection through P2XRs and P2YRs (8). However, the regulation of antiviral innate immune responses by extracellular ATP during viral infection has not been well clarified.

Upon virus infection, the host immune system senses the invading pathogens through cytoplasmic and endosomal pattern recognition receptors (TLRs, NLRs, and RLRs) and releases IFNs with antiviral, immunomodulatory, and antiproliferative activities to evade virus-induced damage (9). Generally, IFNs can be classified into three subtypes: type I (α and β), type II (γ), and type III (λ) (10). Among them, type I IFNs are evolutionarily conserved and consist of α subtypes (14 human, 11 mouse) and single β, ε, κ, τ, ζ, and ω subtypes, which are all important in fighting viral infection (11). Although the subtypes of type I IFNs seem to be determined by pathogen-specific activation of discrete signaling effectors, the type I IFNs are all recognized by IFNAR, which results in the activation of multiple signaling effectors and pathways that coordinate to invoke gene and protein regulation in target cells to create an antiviral response (12). Meanwhile, the inducible production of type I IFN plays a pivotal role in antiviral immune responses through inducing cellular resistance to viral infection and triggering apoptosis of virus-infected cells (13). Furthermore, IFNs are antiviral effectors to both RNA and DNA viruses, as well as are prototypic biological response modifiers for oncology and show effectiveness in suppressing the manifestations of multiple sclerosis (14). Thus, it is crucial to understand the regulation of IFN production in cell-intrinsic antiviral defense.

Although seven P2X subunits have been identified (P2X1–7) (15), the P2X7 receptor is the most important in mediating inflammatory diseases, particularly in neuroinflammation (16). Furthermore, formation of the P2X7 receptor pore is essential for activating the NLRP3 inflammasome (17). P2X7 is also responsible for the release of inflammatory cytokines of the IL-1 family, IL-2, IL-6, and IL-18 (18–20); however, the functions and

*Shanghai Key Laboratory of Regulatory Biology, Institute of Biomedical Sciences and School of Life Sciences, East China Normal University, Shanghai 200241, China; and †Bioray Laboratories Inc., Shanghai 200241, China

ORCID: 0000-0002-5402-6527 (B.D.).

Received for publication February 6, 2017. Accepted for publication June 10, 2017.

This work was supported by the National Natural Science Foundation of China (Grants 31570896, 81272369, and 81672811), the Science and Technology Commission of Shanghai Municipality (Grant 15JC1401500), and the Joint Research Institute for Science and Society (Grant 14JORISS01).

Address correspondence and reprint requests to Dr. Bing Du, Institute of Biomedical Sciences and School of Life Sciences, East China Normal University, 500 Dongchuan Road, Shanghai 200241, China. E-mail address: bdu.ecnu@gmail.com

The online version of this article contains supplemental material.

Abbreviations used in this article: BBG, Brilliant Blue G; BMDM, bone marrow–derived macrophage; CBX, carbenoxolone; FFA, flufenamic acid; MLV, murine leukemia virus; MOI, multiplicity of infection; NDV, Newcastle disease virus; NEM, *N*-ethylmaleimide; PRD, positive regulatory domain; P2XR, P2X receptor; P2YR, P2Y receptor; suramin, suramin hexasodium salt; VSV, vesicular stomatitis virus.

mechanisms of P2X7 in viral infection remain unknown. In this article, we demonstrate that ATP can be highly released by virus-infected cells as a "danger signal." Consequently, extracellular ATP protects the host against DNA and RNA virus infections through facilitating IFN-β expression in P38/JNK/ATF-2 signaling pathways. This kind of protection could be eliminated by P2X7 knockout or P2X7 inhibitors. Therefore, we suggest that ATP/P2X7, which functions as a danger signal, upregulates virus-triggered antiviral innate immune responses by promoting IFN-β production.

Materials and Methods

Mice

C57BL/6 wild-type mice were purchased from the Shanghai Laboratory Animal Company (Shanghai, China). P2X7- and NLRP3-knockout mice were generated by CRISPR/Cas systems. In vitro–transcribed Cas9 mRNA and guide RNA were injected into mouse (C57BL/6) zygotes. Founders of F0 mice with frameshift mutations were screened with a T7E1 assay and validated by DNA sequencing. The target sequences used to generate P2X7-knockout mice were 5′-GGTGACGGAGAATGTCACAG-3′ (site 1) and 5′-TGAGCGATAAGCTGTACCAG-3′ (site 2). Between these two sites, 182 bases were deleted, which contributed to the loss of function of mouse P2X7. The target sequence used to generate NLRP3-knockout mice was 5′-CTGTATCCCAGTCCCCAG-3′; seven bases were deleted on the target, which contributed to the loss of function of mouse NLRP3. All mice were maintained in specific pathogen–free facilities at the Animal Center of East China Normal University. Animal care and use complied with institutional guidelines.

Reagents

An ATP bioluminescence assay kit, carbenoxolone (CBX), *N*-ethylmaleimide (NEM), flufenamic acid (FFA) ATP, suramin hexasodium salt (suramin), Brilliant Blue G (BBG), Bz-ATP, SB203580, SP600125, Apyrase, and A-740003 were purchased from Sigma. RNAiso plus, PrimeScript RT Master Mix, and SYBR Premix Ex Taq were from TaKaRa. A mouse IFN-β ELISA kit was from BioLegend, and a mouse IL-1β ELISA kit was from BD Biosciences. The mouse IFN-α/β receptor block/neutralize polyclonal goat IgG (AF1083) and normal goat IgG control were from R&D Systems. Abs specific to P38, phosphorylated P38, JNK, phosphorylated JNK, IRF3, phosphorylated IRF3, ERK1/2, phosphorylated ERK1/2, IRF7, phosphorylated IRF7, and phosphorylated P65 were from Cell Signaling Technology. Abs specific to ATF-2 and phosphorylated ATF-2 were from ABclonal, Ab specific to P2X7 was from Santa Cruz Biotechnology, and Ab specific to NLRP3 was from Adipogen.

Cell culture

RAW 264.7, L929, HEK-293T, and HeLa cells were obtained from the American Type Culture Collection. RAW 264.7, HEK-293T, and HeLa cells were cultured in DMEM containing 10% FBS and 1% penicillin/streptomycin, whereas L929 cells were grown in RPMI 1640 containing 10% FBS and 1% penicillin/streptomycin. For bone marrow–derived macrophages (BMDMs), bone marrow cells were collected from tibias and femurs by flushing with DMEM. The cell suspension was filtered through a 40-μm cell strainer to remove any cell clumps and cultured in DMEM containing 10% FBS, 1% penicillin/streptomycin, and L929 culture supernatants.

ATP-release assay

RAW 264.7 cells (2×10^5 cells per well) or L929 cells (1×10^5 cells per well) were plated in 24-well plates overnight, and the cells were infected with vesicular stomatitis virus (VSV) for different amounts of time. ATP release in supernatants from cell cultures was detected using an ATP bioluminescence assay kit (Sigma-Aldrich, St. Louis, MO), according to the manufacturer's protocol. For ATP release in vivo, mice were injected i.p. with VSV (5×10^9 PFU/kg) and sacrificed 24 h later, peritoneal cavities were washed with 400 μl of PBS, and ATP levels were detected as described above.

Real-time PCR

Cells were dissolved in RNAiso plus (TaKaRa). cDNA was synthesized from extracted total RNA using the PrimeScript RT Master Mix Perfect Real Time kit (TaKaRa), according to the manufacturer's protocol. Quantitative PCR was performed using SYBR Green premix (TaKaRa); 500 ng of cDNA was used as a template. The following primers were used: human IFN-β, 5′-GGATGAACTTTGACATCCCT-3′ (forward) and 5′-ATAGACATTAGCCAGGAGGT-3′ (reverse); mouse IFN-β, 5′-CAGCTCCAAGAAAGGACGAAC-3′ (forward) and 5′-GGCAGTGTAACTCTTCTGCAT-3′ (reverse); Newcastle disease virus (NDV), 5′-TATACACCTCATCTCAGACAGGGTCAATCA-3′ (forward) and 5′-GCTCTCTTTAAGTCGGAGGATGTTGGC-3′ (reverse); mouse IFN-α, 5′-CGCAGGAGAAGGTGGATGCCCAG-3′ (forward) and 5′-CAGCACATTGGCAGAGGAAGACAGG-3′ (reverse); VSV Indiana serotype, 5′-ACGGCGTACTTCCAGATGG-3′ (forward) and 5′-CTCGGTTCAAGATCCAGGT-3′ (reverse); mouse P2X7, 5′-CGTGCACACCAAGGTCAAAG-3′ (forward) and 5′-CACCCCTTTTTACAACGCCG-3′ (reverse); and β-actin, 5′-GTACGCCAACACAGTGCTG-3′ (forward) and 5′-CGTCATACTCCTGCTTGCTG-3′ (reverse). β-actin was used as an internal control gene.

MTS assay

RAW 264.7 cells (2×10^4 cells per well) and 293T cells (8×10^3 cells per well) were plated in 96-well plates overnight and then treated as indicated in the figure legends for 24 h. Twenty microliters of MTS (Promega) was added to each well and incubated for 1 h at 37°C. After incubation, the absorption was measured at 490 nm. Cell viability of the untreated group was normalized to 100%.

Crystal violet staining assay

293T cells (8×10^3 cells per well) were seeded into 96-well plates overnight. The cells were treated with ATP for 6 h and then infected with VSV (multiplicity of infection [MOI] = 0.01) or HSV (MOI = 0.01) for 12 h. The medium was removed, and the cells were fixed with 4% paraformaldehyde in PBS for 20 min at room temperature. Following this, 20 μl of crystal violet stain was added to each well for 30 min, and cells were washed with PBS five times before photographs were taken.

Luciferase assay

293T cells (1×10^5 cells per well) were seeded into 24-well plates overnight and cotransfected with 800 ng of IFN-β promoter luciferase expression vectors and 50 ng of *Renilla* luciferase expression vectors for 24 h by calcium phosphate transfection. The cells were treated with ATP or VSV (MOI = 0.01) for 12 h. Luciferase activity was measured with a Dual-Luciferase Assay System, and the results were normalized by *Renilla* activity.

Immunofluorescence

Mice were anesthetized with ketamine/rompun, treated with 5 mg/kg ATP through nasal dripping for 6 h, and infected intranasally with VSV (5×10^9 PFU/kg) for 24 h. Mice were sacrificed, and the olfactory bulbs were fixed with 4% paraformaldehyde in PBS overnight and cut into 8-μm slices. After permeabilization with 0.1% Triton X-100, tissue was blocked with 5% BSA and stained with anti–VSV-G Ab and Alexa Fluor 488–conjugated secondary Ab. DAPI was used to stain nuclei.

ELISA

BMDMs were plated in 24-well plates (2×10^5 cells per well) and treated with ATP for 12 h. IFN-β production was measured using a Mouse IFN-β ELISA kit (BioLegend), according to the manufacturer's instructions.

Western blotting

After stimulation, cells were lysed in 1× SDS loading buffer. Lysates were separated by 10% SDS-PAGE, transferred to nitrocellulose membranes, and blocked with 5% BSA. The proteins were hybridized with various primary Abs and incubated with the appropriate fluorescent secondary Abs. Protein bands were visualized using the Odyssey laser digital imaging system (Gene Company).

H&E staining

Organs from $P2X7^{+/+}$ and $P2X7^{-/-}$ mice were dissected, fixed with 4% paraformaldehyde in PBS overnight, embedded into paraffin, cut into slices, and stained with H&E solution. Histologic structures were examined by light microscopy.

Statistical analysis

Data are shown as mean ± SD. The Student *t* test (two-tailed) was used to analyze the significance of data, and $p < 0.05$ was considered statistically significant.

Results

Extracellular ATP is highly increased in viral infection

To investigate the potential role of ATP as a danger signal in viral infection, we detected the release of endogenous ATP in VSV-infected RAW 264.7 (Fig. 1A) and L929 (Fig. 1B) cells. Extracellular ATP in VSV-infected cell supernatant was clearly increased in a time-dependent manner. Consequently, we explored the reason why ATP is released from virus-infected cells by different inhibitors of plasma membrane channels, including CBX (a pannexin channel inhibitor), NEM (an inhibitor of vesicular exocytosis), and FFA (a gap junction inhibitor). As shown in Fig. 1C, the release of ATP is blocked by NEM and CBX but is influenced little by FFA. These data indicate that VSV-induced ATP release occurs through pannexin channels (long term) and vesicular exocytosis (short term), which is consistent with the accumulation of ATP in the virus-infected cell supernatant. Accordingly, we also observed a dramatic increase in ATP in the abdomen of mice infected with VSV i.p. (Fig. 1D). Taken together, our data suggested that ATP release is a common phenomenon in virus infection in vitro and in vivo.

Extracellular ATP protects cells from VSV infection

To further elucidate the potential of extracellular ATP in fighting against viral infection, we assessed viral RNA replication and cell viability in ATP-treated cells. Surprisingly, the RNA replication of VSV in ATP-treated RAW 264.7 cells was reduced significantly in a time-dependent (Fig. 2A) and concentration-dependent (Fig. 2B) manner. Accordingly, the cell viability of VSV-infected RAW 264.7 and 293T cells was enhanced by ATP in a concentration-dependent manner (Fig. 2C), indicating that extracellular ATP plays an important role in protecting virus-infected cells. Similar results were observed in 293T cells; cytopathic effects were induced by VSV, as determined using a crystal violet staining assay (Fig. 2D). However, the cell viability was little changed in uninfected RAW 264.7 and 293T cells at low concentration, indicating that protection by ATP in viral infection is independent of cell proliferation (Fig. 2E). Meanwhile, we also observed increased viability with 200 and 400 μM ATP in 293T cells, suggesting that the ATP-increased cell viability could account, in part, for ATP-mediated protection in VSV infection. To determine the protective role of virus-triggered ATP, we treated cells with apyrase to hydrolyze endogenous extracellular ATP; accordingly, VSV RNA replication was increased in apyrase-treated cells (Fig. 2F). Thus, these data show the positive regulation of antiviral responses by ATP in VSV infection.

Extracellular ATP exhibits antiviral activities in RNA and DNA virus

To confirm the antiviral activities of ATP in a broad-spectrum virus, we treated NDV-, murine leukemia virus (MLV)-, VSV-, and HSV-infected cells with different concentrations of ATP. As shown in Fig. 3A, GFP^+ 293T cells were reduced in ATP-treated cells, indicating that NDV-GFP infection is restricted by ATP. Consequently, RNA replication of NDV-GFP is also reduced by ATP (Fig. 3B). Meanwhile, we infected HeLa (Fig. 3C) and 293T (Fig. 3D) cells with MLV-GFP, which is different from VSV and NDV, because MLV is a positive-sense ssRNA virus. Similarly, the proportion of GFP^+ cells was significantly decreased by ATP in a concentration-dependent manner. In the same way, when HeLa and 293T cells were infected with VSV-GFP, GFP^+ cells were also reduced by ATP (Fig. 3E). Finally, we also infected 293T cells with the DNA virus HSV. As shown in Fig. 3F, HSV-induced cell cytopathic effects were eliminated by ATP in a concentration-dependent manner. Taken together, these data suggest that ATP has broad-spectrum antiviral activities, which have great potential in protecting hosts from viral infection.

Extracellular ATP-mediated antiviral activities are dependent on P2X7

It is well known that extracellular ATP can activate G protein–coupled P2YRs and ionotropic P2XRs. Thus, to explore the mechanisms of ATP-mediated antiviral activities, we treated VSV-infected cells with ATP, with or without suramin (inhibitor of GPCRs) and BBG (specific inhibitor of P2X7). As shown in Fig. 4A and 4B, protection of 293T and RAW 264.7 cells by ATP was little changed by suramin, suggesting that ATP-mediated antiviral activities are independent of GPCRs. Conversely, ATP-reduced VSV RNA replication was blocked by BBG in a concentration-dependent manner (Fig. 4C, 4D), with little

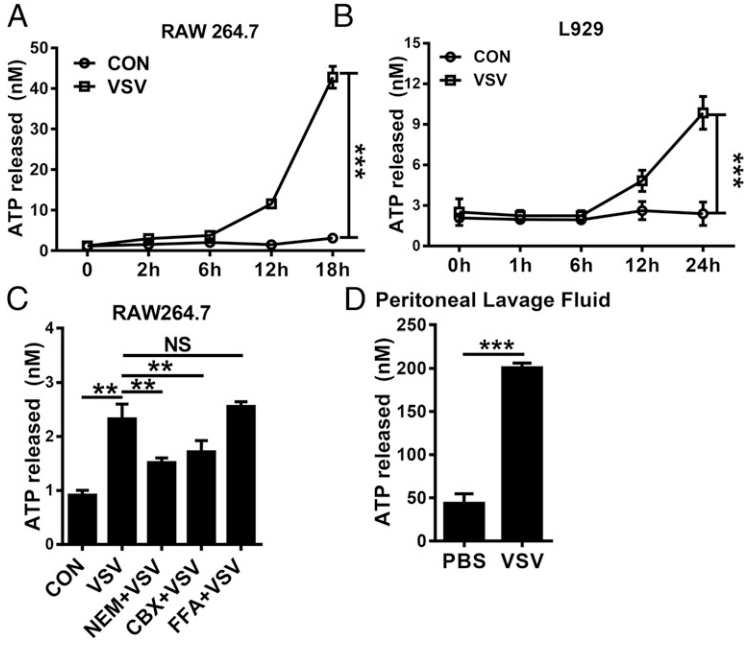

FIGURE 1. VSV infection results in ATP release from cells and mice. RAW 264.7 cells were infected with VSV (MOI = 0.01) (**A**), and L929 cells were infected with VSV (MOI = 1) (**B**), and levels of extracellular ATP were measured at the indicated times. (**C**) RAW 264.7 cells were pretreated or not with NEM (5 μM), CBX (5 μM), or FFA (10 μM) 30 min before being infected with VSV (MOI = 0.01) for 2 h, and ATP release was measured. (**D**) Mice were injected i.p. with PBS or VSV (5×10^9 PFU/kg) for 24 h, and ATP release was measured. Data are shown as mean ± SD. $^{**}p < 0.01$, $^{***}p < 0.001$.

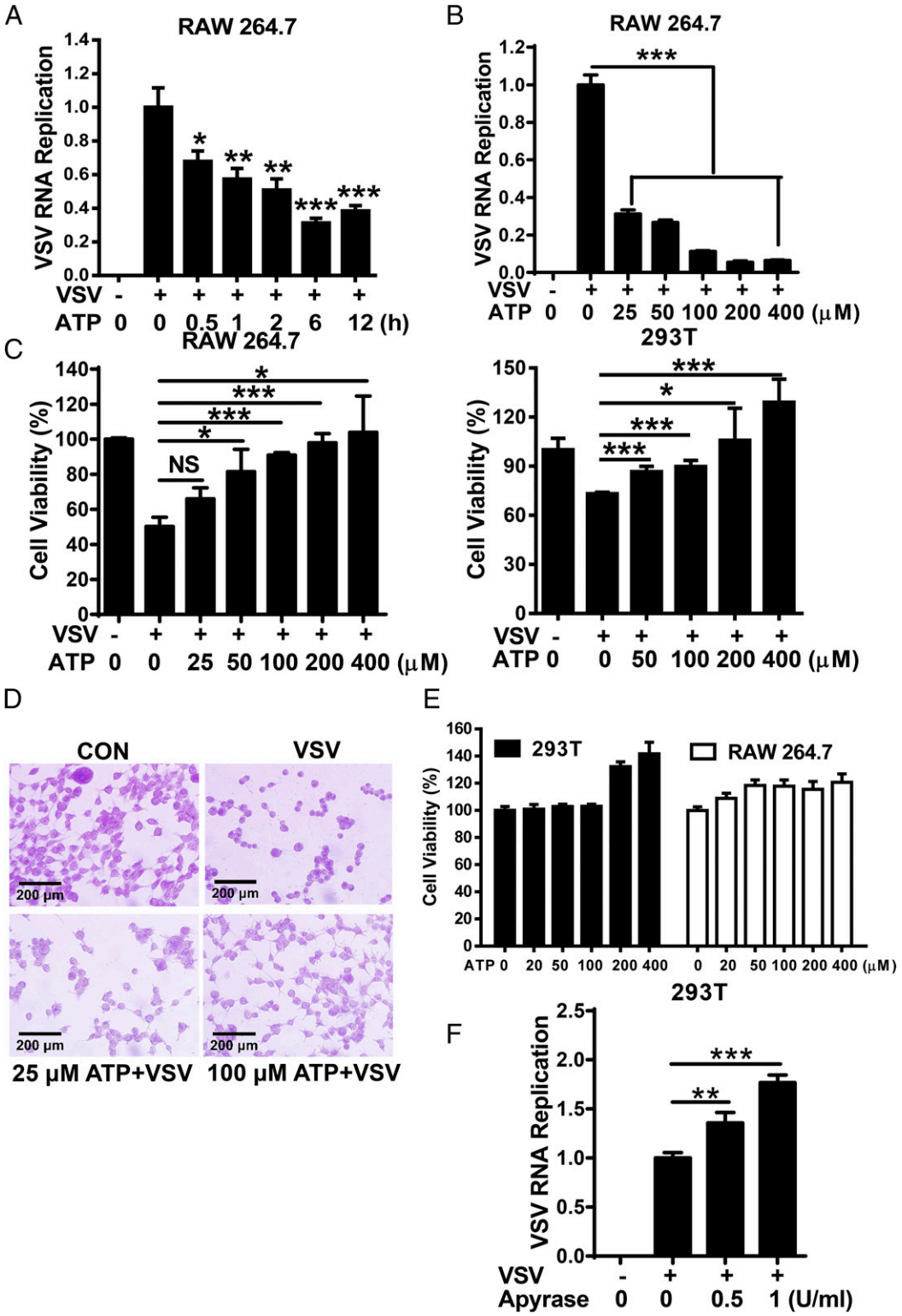

FIGURE 2. ATP protects cell lines against VSV infection. (**A**) RAW 264.7 cells were treated with 100 μM ATP for different lengths of time and then cells were infected with VSV (MOI = 0.01) for 12 h. VSV RNA replicates were measured by quantitative RT-PCR (qRT-PCR). (**B**) RAW 264.7 cells were treated for 6 h with various concentration of ATP and then infected with VSV (MOI = 0.01) for 12 h. VSV RNA replicates were measured by qRT-PCR. (**C**) RAW 264.7 cells and 293T cells were treated for 6 h with various concentration of ATP and then infected with VSV (MOI = 0.01) for 24 h. Cell viability was detected by MTS assay. (**D**) 293T cells were treated with ATP (25 or 100 μM) for 6 h. Then cells were infected with VSV (MOI = 0.01) for 12 h, stained with crystal violet, and observed under a microscope. (**E**) 293T cells and RAW 264.7 cells were treated with 25–400 μM ATP for 24 h. Cell viability was detected by MTS assay. (**F**) 293T cells were treated with 0.5 or 1 U/ml apyrase for 1 h and then infected with VSV (MOI = 0.01) for 12 h. VSV RNA replicates were measured by qRT-PCR. Data are shown as mean ± SD. $*p < 0.05$, $**p < 0.01$, $***p < 0.001$.

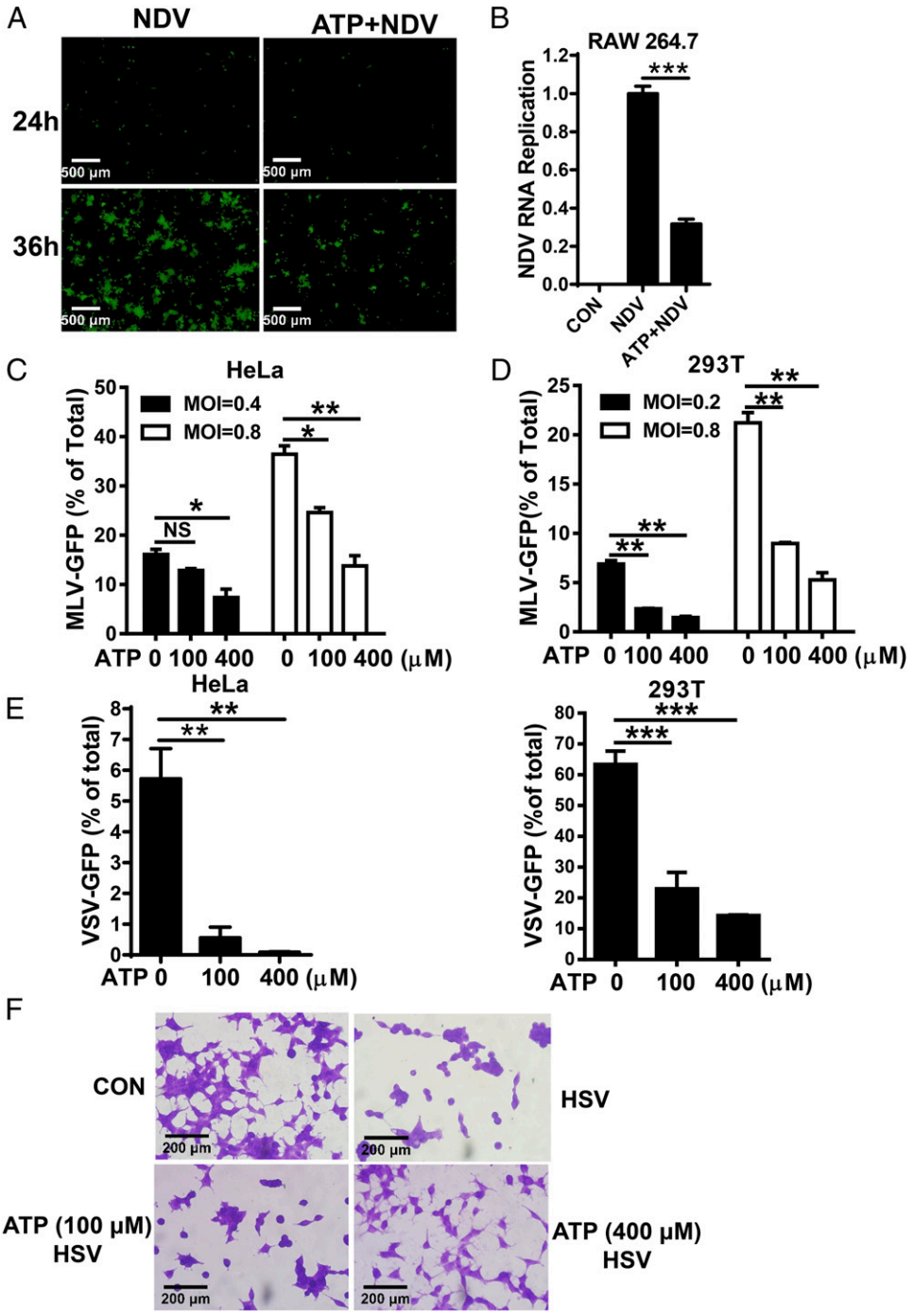

FIGURE 3. ATP protects cells against RNA and DNA virus infection. (**A**) 293T cells were treated with 100 μM ATP for 6 h, infected with NDV-GFP (MOI = 0.01) for 24 or 36 h, and observed under a microscope. (**B**) RAW 264.7 cells were treated with 100 μM ATP for 6 h and then infected with NDV-GFP (MOI = 0.01) for 12 h. NDV RNA replicates were measured by quantitative RT-PCR. (**C**) HeLa cells were treated with 100 or 400 μM ATP for 6 h and then cells were infected with MLV-GFP (MOI = 0.4 or 0.8) for 24 h. Cells containing GFP were analyzed by FACS. (**D**) 293T cells were treated with 100 or 400 μM ATP for 6 h and then cells were infected with MLV-GFP (MOI = 0.2 or 0.8) for 24 h. Cells containing GFP were analyzed by FACS. (**E**) HeLa cells and 293T cells were treated with 100 or 400 μM ATP for 6 h and then infected with VSV-GFP (MOI = 0.01 and 0.005, respectively) for 24 h. Cells containing GFP were analyzed by FACS. (**F**) 293T cells were treated with 100 or 400 μM ATP for 6 h and then infected with HSV (MOI = 0.01) for 12 h. Cells were stained with crystal violet and observed under a microscope. Data are shown as mean ± SD. $^{*}p < 0.05$, $^{**}p < 0.01$, $^{***}p < 0.001$.

influence on cell viability (Fig. 4E), implying that ATP could protect cells from virus infection through P2X7. Similar data were also observed in 293T cells treated with A-740003 (selective P2X7 receptor antagonist) (Fig. 4F). Furthermore, we treated the cells with the P2X7-specific agonist, BZATP. As shown in Fig. 4G, BZATP has a similar role to ATP in restricting VSV RNA replication. To further confirm that ATP-mediated antiviral activities are dependent on the P2X7 receptor, P2X7-knockout mice were generated. RT-PCR and Western blot results showed that P2X7 was deleted in the P2X7-knockout mice (Fig. 4H, Supplemental Fig. 1A–C). Meanwhile, the ATP-activated NLRP3 inflammasome was eliminated in P2X7-knockout BMDMs, suggesting that the construction of P2X7-knockout mice was successful (Supplemental Fig. 1D). H&E staining revealed that the tissue architecture of olfactory bulbs, liver, spleen, and lung were all little changed in P2X7 receptor–knockout mice (Supplemental Fig. 1E). We then determined that ATP-reduced VSV RNA replication was completely eliminated in P2X7-knockout BMDMs. These results demonstrate that ATP-mediated antiviral activities occur primarily through the P2X7 receptor.

Extracellular ATP-mediated protection is eliminated in P2X7-deficient mice

To further investigate the protective role of ATP in an animal model, we challenged wild-type and P2X7-deficient mice with VSV, with or without ATP. As shown in Fig. 5A, the distribution of VSV in spleen, lung, and liver was decreased in ATP-treated mice. This type of restriction was eliminated in P2X7-knockout mice, suggesting an exclusive role for P2X7 in ATP-mediated antiviral activities. Furthermore, when mice were challenged i.p. with a

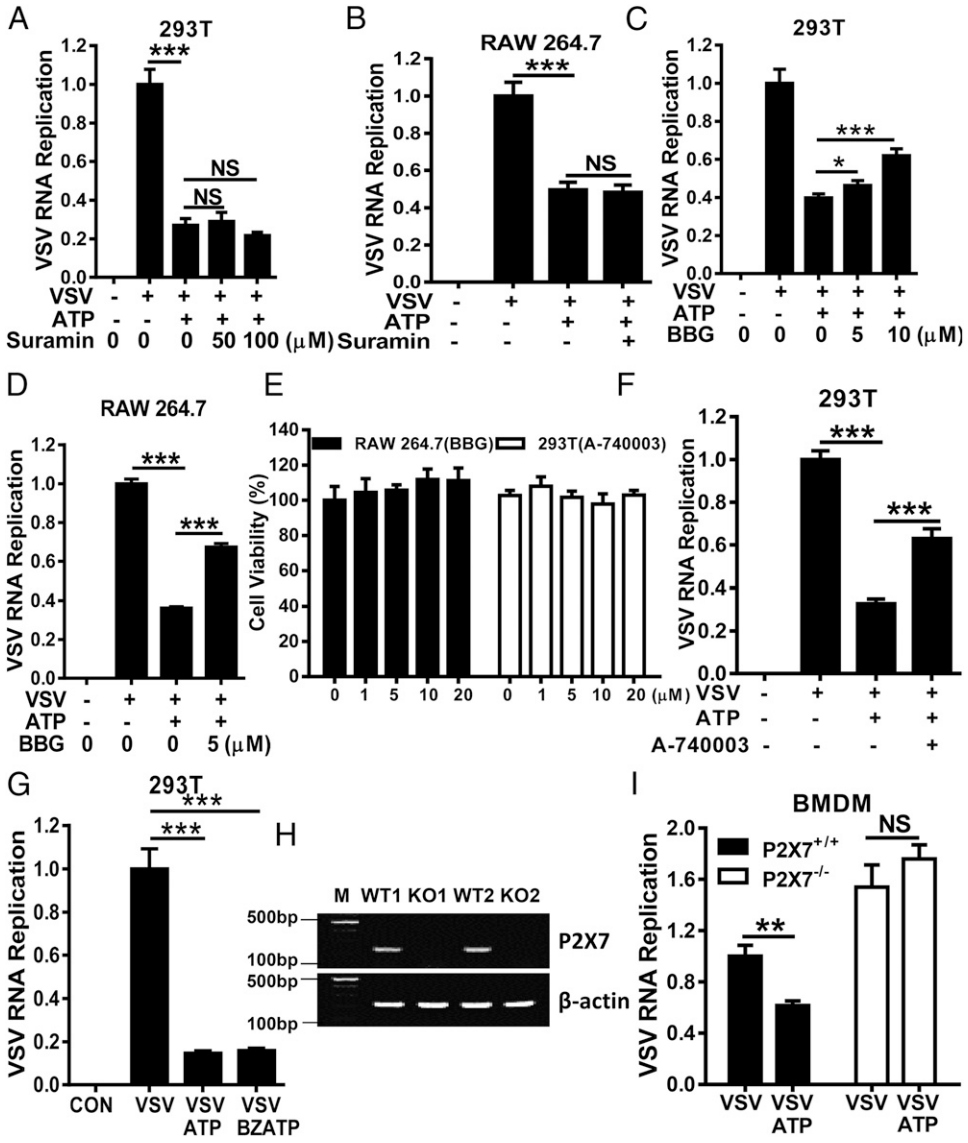

FIGURE 4. ATP protects cells against virus infection through the P2X7 receptor. 293T (**A**) or RAW 264.7 (**B**) cells were treated or not with various concentration of suramin for 30 min before being exposed to 100 μM ATP for 6 h. Then cells were infected with VSV (MOI = 0.01) for 12 h. VSV RNA replicates were measured by quantitative RT-PCR (qRT-PCR). 293T (**C**) or RAW 264.7 (**D**) cells were treated or not with BBG (5 or 10 μM) for 30 min before being exposed to 100 μM ATP for 6 h. Then cells were infected with VSV (MOI = 0.01) for 12 h. VSV RNA replicates were measured by qRT-PCR. (**E**) RAW 264.7 cells were treated with various concentrations of BBG, and 293T cells were treated with various concentration of A-740003; cell viability was detected by MTS assay 24 h later. (**F**) 293T cells were pretreated or not with 10 μM A-740003 for 1 h before being treated with 100 μM ATP for 6 h. Then cells were infected with VSV (MOI = 0.01) for 12 h. VSV RNA replicates were measured by qRT-PCR. (**G**) 293T cells were treated with 100 μM ATP or BZATP for 6 h and then infected with VSV (MOI = 0.01) for 12 h. VSV RNA replicates were measured by qRT-PCR. (**H**) P2X7 expression in $P2X7^{+/+}$ and $P2X7^{-/-}$ BMDMs was detected by RT-PCR. (**I**) $P2X7^{+/+}$ or $P2X7^{-/-}$ BMDMs were treated with 100 μM ATP for 6 h. Then cells were infected with VSV (MOI = 1) for 12 h. VSV RNA replicates were measured by qRT-PCR. Data are shown as mean ± SD. $*p < 0.05$, $**p < 0.01$, $***p < 0.001$.

lethal dose of VSV, the survival of ATP-treated wild-type mice was increased significantly, but there was little change in that of P2X7-deficient mice (Fig. 5B). VSV is a neurotropic virus capable of accessing or entering the nervous system and is transmitted directly via the transcutaneous or transmucosal route. Thus, to mimic the natural infection of VSV, we intranasally infected wild-type and P2X7-knockout mice, with or without ATP, to detect the distribution of VSV in olfactory bulbs, which is consistent with i.p. infection data. The RNA replication of VSV in olfactory bulbs was significantly decreased by ATP in wild-type mice but not in P2X7-knockout mice (Fig. 5C). Similar data were observed in the immunofluorescence assay (Fig. 5D). In conclusion, extracellular ATP has great potential in protecting the host from viral infection through P2X7, suggesting a potential therapeutic role for ATP/P2X7 in preventing viral diseases.

ATP facilitates IFN-β production in virus infection

To elucidate the mechanism of ATP/P2X7-mediated antiviral activity, we detected the expression of type I IFN in ATP-treated cells. When we treated BMDMs (Fig. 6A), 293T cells (Fig. 6B), and RAW 264.7 cells (Fig. 6C) with ATP at the indicated times, RNA expression of IFN-β was increased significantly, which is consistent with the antiviral activities of ATP, whereas the expression of IFN-α was little changed. Accordingly, the transcriptional activity of the IFN-β promoter can also be enhanced by ATP in a concentration-dependent manner (Fig. 6D). In addition,

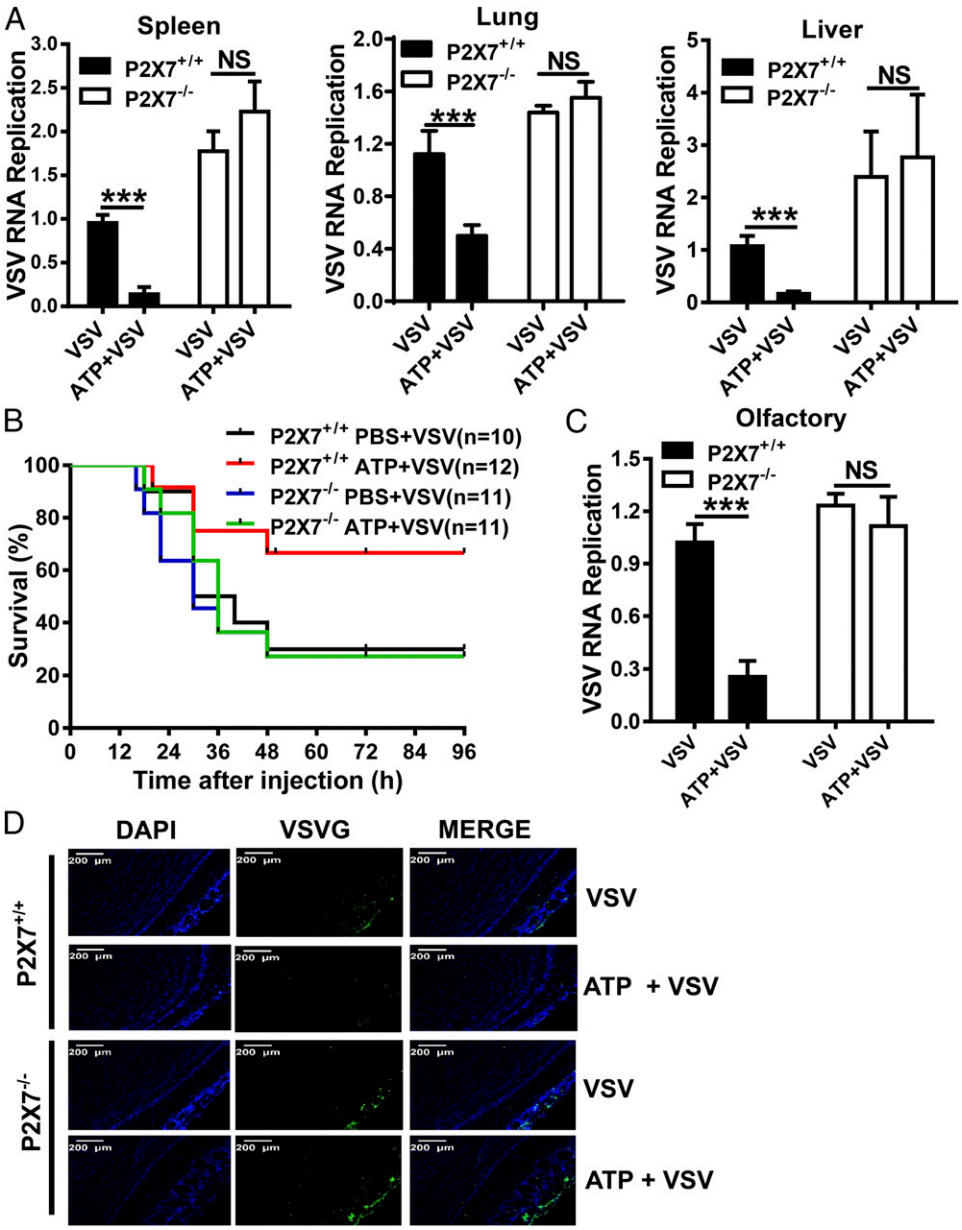

FIGURE 5. ATP protects mice against virus infection through the P2X7 receptor. (**A**) Six-week-old $P2X7^{+/+}$ and $P2X7^{-/-}$ mice (n = 3 or 4 per group) were treated i.p. with 50 mg/kg ATP for 6 h and then infected i.p. with VSV (5×10^9 PFU/kg) for 24 h. VSV RNA replicates in organs were measured by quantitative RT-PCR. (**B**) Six-week-old $P2X7^{+/+}$ and $P2X7^{-/-}$ mice were treated i.p. with 50 mg/kg ATP for 6 h and then injected i.p. with VSV (5×10^{10} PFU/kg). Mice survival was recorded for 96 h. (**C**) $P2X7^{+/+}$ and $P2X7^{-/-}$ mice (n = 4 per group) were treated with 5 mg/kg ATP through nasal dripping for 6 h and then intranasally infected with VSV (5×10^9 PFU/kg) for 24 h. VSV RNA replicates in olfactory bulbs were measured by quantitative RT-PCR. (**D**) $P2X7^{+/+}$ and $P2X7^{-/-}$ mice were treated with 5 mg/kg ATP through nasal dripping for 6 h and then intranasally infected with VSV (5×10^9 PFU/kg) for 24 h. VSV presence in olfactory bulbs was detected by immunofluorescence. Scale bars, 200 μm. Data are shown as mean ± SD. ***$p < 0.001$.

ATP-increased IFN-β mRNA expression can be blocked by the P2X7-specific inhibitor BBG and A-740003 (Fig. 6E, 6F). Furthermore, RNA (Fig. 6G) and protein (Fig. 6H) expression levels of IFN-β were enhanced by ATP in wild-type, but not in P2X7-knockout, BMDMs. Moreover, when the activity of IFN-β was blocked with the anti-IFNR Ab, ATP-mediated inhibition of VSV replication was eliminated, suggesting a key role for IFN-β in ATP-mediated antiviral activities (Fig. 6I). To assess whether the classical NLRP3/IL-1 pathway is involved in ATP-mediated antiviral activities, RNA replication of VSV in ATP-treated wild-type and P2X7-knockout BMDMs was determined. VSV infection in ATP-treated NLRP3-knockout BMDMs is almost the same as in ATP-treated wild-type BMDMs (Supplemental Fig. 2), suggesting that ATP-mediated antiviral activities are independent of the NLRP3/IL-1β pathway.

ATP activates P38/JNK/ATF-2–associated signaling pathways

Transcriptional regulation of IFN-β requires the activation of different transcription factors, such as IRF3/IRF7, NF-κB, ERK, and ATF-2/c-Jun. Therefore, we assessed their signaling in ATP-treated or P2X7-knockout cells by Western blotting (Fig. 7, Supplemental Fig. 3). As shown in Fig. 7A, only the phosphorylation of ATF2 was increased by ATP; IRF3, IRF7, P65, and ERK signaling was little changed. Furthermore, when P2X7-knockout cells were treated with ATP, the phosphorylation of ATF2 was little changed (Fig. 7B). In addition, ATP-dependent ATF-2 phosphorylation was strongly prevented by the P38- and JNK-specific inhibitors (Fig. 7C). Consequently, ATP-enhanced IFN-β RNA expression can also be eliminated by P38- and JNK-specific inhibitors (Fig. 7D), implying a dominant role for P38 and JNK signaling in ATP-increased IFN-β production and protection. These data demonstrate that ATP-induced IFN-β production occurs primarily through P38/JNK and ATF-2 signaling pathways, which can protect cells from viral infection.

Discussion

In reaction to invading pathogens, the host orchestrates inflammatory responses through the activation of pattern recognition receptors. As part of this process, purinergic signaling contributes to the facilitation of innate and acquired immune responses to

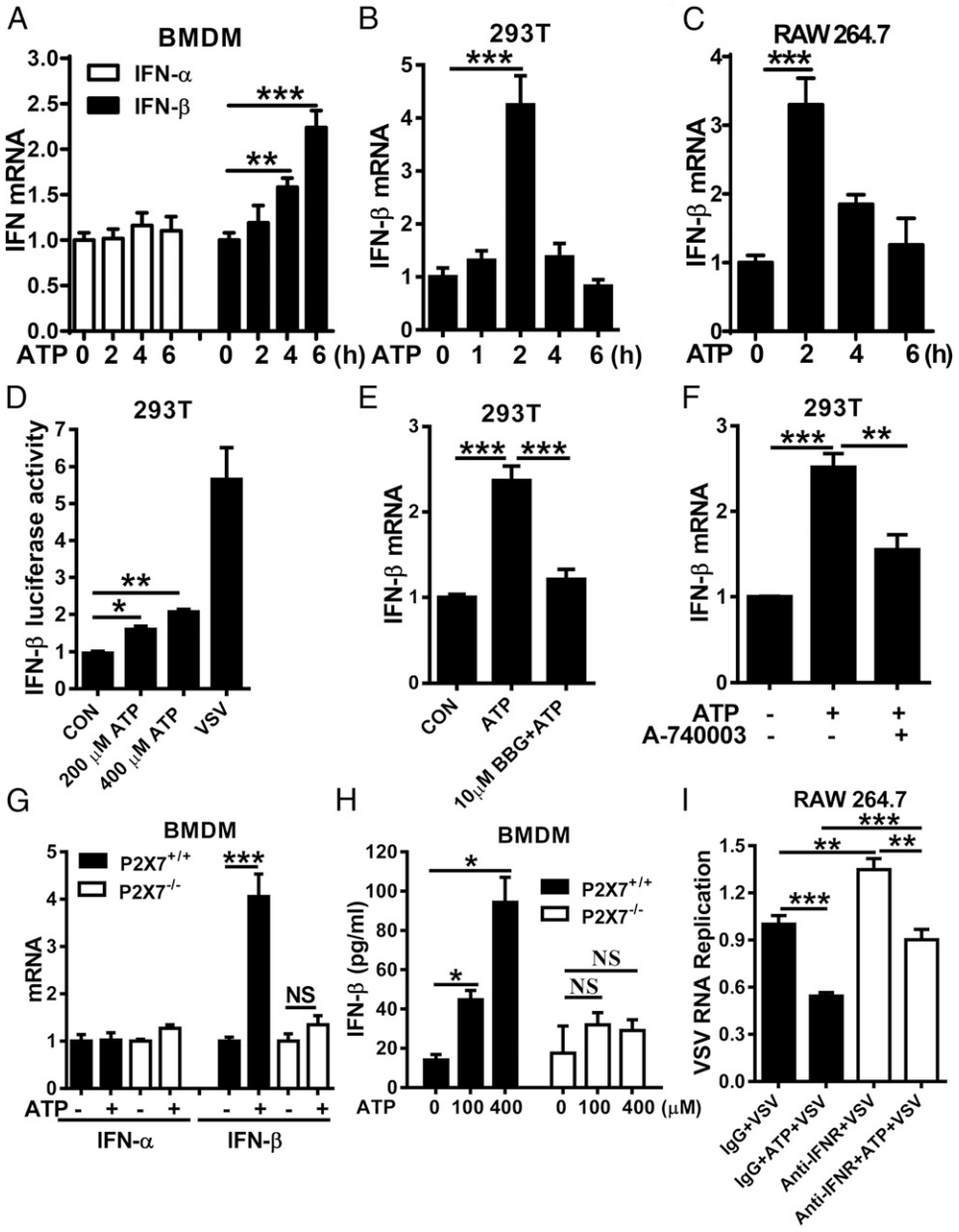

FIGURE 6. ATP protects cells against virus infection through upregulating IFN-β expression. (**A**) BMDMs were stimulated with 100 μM ATP for the indicated times. IFN-α and IFN-β mRNA expression were measured by quantitative RT-PCR (qRT-PCR). 293T (**B**) and RAW 264.7 (**C**) cells were treated with 100 μM ATP for the indicated times, and IFN-β mRNA expression was measured by qRT-PCR. (**D**) 293T cells were transiently cotransfected with the IFN-β promoter and *Renilla* luciferase expression vectors for 24 h and then cells were stimulated with 200 or 400 μM ATP for 12 h. Luciferase activity was measured with a Dual-Luciferase Assay System. 293T cells were pretreated or not with 10 μM BBG for 30 min (**E**) or 10 μM A-740003 for 1 h (**F**) before being exposed to 100 μM ATP for 2 h. IFN-β mRNA expression was measured by qRT-PCR. (**G**) $P2X7^{+/+}$ and $P2X7^{-/-}$ BMDMs were stimulated with 100 μM ATP for 6 h, and IFN-α and IFN-β mRNA expression was measured by qRT-PCR. (**H**) $P2X7^{+/+}$ and $P2X7^{-/-}$ BMDMs were exposed to 100 or 400 μM ATP for 12 h, and IFN-β production was detected by ELISA. (**I**) RAW 264.7 cells were pretreated or not with anti–IFN-α/β receptor IgG for 3 h before being treated with 100 μM ATP for 6 h. Thereafter, cells were infected with VSV (MOI = 0.01) for 12 h. VSV RNA replicates were measured by qRT-PCR. Data are shown as mean ± SD. $*p < 0.05$, $**p < 0.01$, $***p < 0.001$.

eliminate the potential damage from pathogens. Previous studies have shown that nucleotides, such as ATP, UTP, and UDP, could be released through multiple plasma membrane channels during different stages of infection (8, 21). Moreover, the spatial and temporal release pattern of endogenous danger signals suggests different roles in the fight against invading pathogens. In this study, we observed a persistent accumulation of ATP for 24 h in a virus-infected cell supernatant, even though ATP can be hydrolyzed quickly by extracellular phosphohydrolase. ATP release begins during the early stages of infection, which is different from pathogen-induced cytokines. Thus, the released ATP could serve as a danger signal to alarm the immune system to fight against invading pathogens. Accordingly, we observed a significant increase in IFN-β in ATP-treated cells via the P2X7 receptor, suggesting a dominant role for ATP/P2X7 in the regulation of innate immune responses to viral infection.

Although P2X7 is expressed by many kinds of tissues, the P2X7 receptor is highly and constitutively expressed in cells of hematopoietic lineage and can mediate cell death, the elimination of infected cells, and the regulation of inflammatory responses (22, 23). Under normal conditions, P2X7 activity is restricted to low levels by extracellular divalent cations, such as Ca^{2+} and Mg^{2+}, which alter the affinity of ATP binding in an allosteric manner (24). However, cell stress, such as inflammation or infection, upsets this balance by decreasing the extracellular concentrations of Ca^{2+} and Mg^{2+}, which, combined with an increase in ATP, activates the P2X7 receptor (25). It has been demonstrated that activation of P2X7 triggers many cellular signaling pathways depending on cell type, including the MAPK pathway (26), stress-activated protein kinase pathway (27), phospholipase D (28) and inflammasome activation (29). In this study, we only observed a significant increase in P38 activation in ATP-treated BMDMs. However, phosphorylation of P65, which is involved in NF-κB signaling, was little influenced, even though it is regarded as a key regulator of inflammation, suggesting that ATP-increased IFN-β production is independent of NF-κB signaling.

The induction of IFN-α/β is tightly controlled by essential transcription factors, such as IRF-3 and IRF-7. Accordingly, the

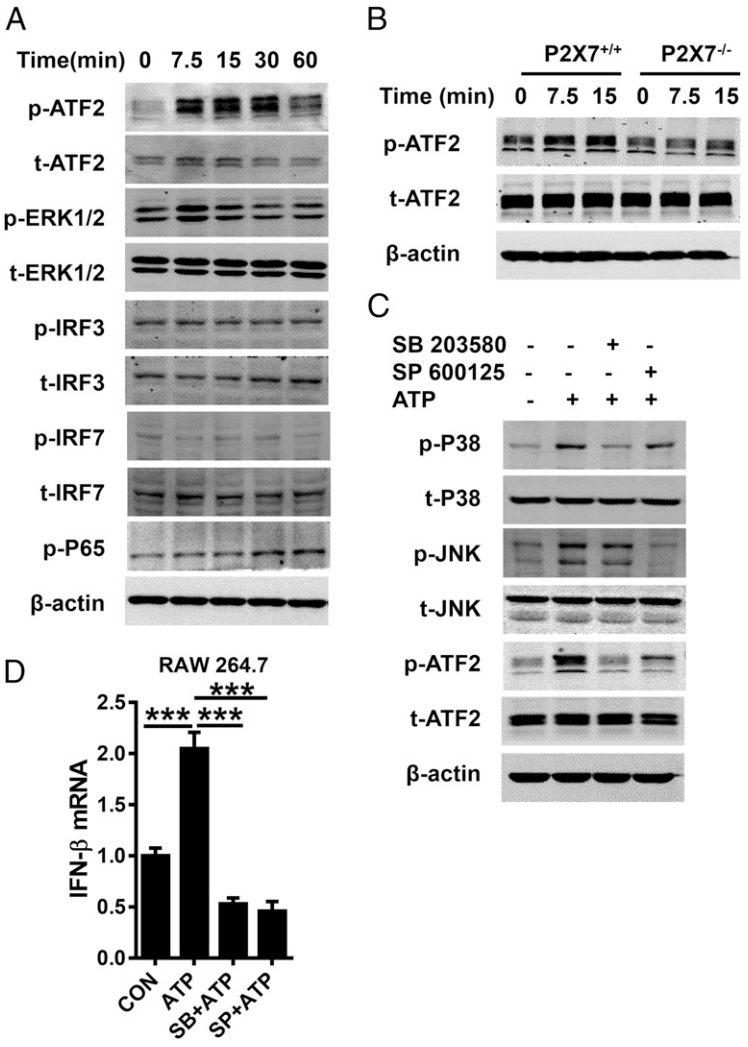

FIGURE 7. ATP upregulates IFN-β expression through the AP-1 signaling pathway. (**A**) BMDMs were treated with 200 μM ATP for the indicated times. Phosphorylated or total proteins involved in regulating IFN-β expression were detected by Western blot. (**B**) *P2X7*$^{+/+}$ and *P2X7*$^{-/-}$ BMDMs were treated with 200 μM ATP for 7.5 or 15 min, and phosphorylated or total ATF-2 was detected by Western blot. (**C**) BMDMs were pretreated with SB 203580 (20 μM) or SP 600125 (20 μM) for 1 h and then treated with 200 μM ATP for 10 min. Phosphorylated or total P38, JNK, and ATF-2 were detected by Western blot. (**D**) RAW 264.7 cells were pretreated with SB 203580 (20 μM) or SP 600125 (20 μM) for 1 h and then treated with 200 μM ATP for 2 h. IFN-β mRNA expression was measured by quantitative RT-PCR. Data are shown as mean ± SD. ***$p < 0.001$.

induction of IFN-α/β is eliminated in IRF-3 and IRF-7 double-knockout mice (30). Therefore, we assessed the phosphorylation of IRF3, IRF7, and P65 in the ATP-treated BMDMs. Surprisingly, all were influenced by ATP to some extent. The core promoter region of IFN-β is composed of four positive regulatory domains (PRDs): PRD I, PRD II, PRD III, and PRD IV (30). PRD IV is tightly regulated by the AP-1 heterodimer of ATF-2 and c-Jun, which is different from other PRDs bound by IRF3/IRF7 or p50/RelA. We then assessed the influence of ATP on ATF-2 signaling. Consistent with the activation of P38, phosphorylation of ATF-2 was increased, implying that AP-1 is the key regulator in ATP-mediated antiviral responses. Although AP-1 plays important, but nonessential, roles in viral induction of IFN-β (31), it is essential for constitutive IFN-β production. c-Jun occupies PRD IV on the IFN-β promoter in uninfected cells, and its deletion decreases constitutive IFN-β expression by half (32). Thus, these data suggested that ATP/P2X7 may be involved in modulating constitutive IFN-β production, which is essential in IFN-mediated homeostasis. Taken together, our study extends the novel function of ATP/P2X7 as a danger signal in antiviral immune responses through P38/ATF-2 signaling and suggests that the ATP/P2X7-associated signaling pathway could have potential therapeutic significance in viral infection, as well as diseases impacted by IFN-β.

Disclosures

The authors have no financial conflicts of interest.

References

1. Matzinger, P. 1994. Tolerance, danger, and the extended family. *Annu. Rev. Immunol.* 12: 991–1045.
2. Seong, S. Y., and P. Matzinger. 2004. Hydrophobicity: an ancient damage-associated molecular pattern that initiates innate immune responses. *Nat. Rev. Immunol.* 4: 469–478.
3. Russo, M. V., and D. B. McGavern. 2015. Immune surveillance of the CNS following infection and injury. *Trends Immunol.* 36: 637–650.
4. Khakh, B. S., and G. Burnstock. 2009. The double life of ATP. *Sci. Am.* 301: 84–90, 92.
5. Junger, W. G. 2011. Immune cell regulation by autocrine purinergic signalling. *Nat. Rev. Immunol.* 11: 201–212.
6. Kellerman, D., R. Evans, D. Mathews, and C. Shaffer. 2002. Inhaled P2Y2 receptor agonists as a treatment for patients with cystic fibrosis lung disease. *Adv. Drug Deliv. Rev.* 54: 1463–1474.
7. Amisten, S., O. Melander, A. K. Wihlborg, G. Berglund, and D. Erlinge. 2007. Increased risk of acute myocardial infarction and elevated levels of C-reactive protein in carriers of the Thr-87 variant of the ATP receptor P2Y11. *Eur. Heart J.* 28: 13–18.
8. Ren, H., Y. Teng, B. Tan, X. Zhang, W. Jiang, M. Liu, W. Jiang, B. Du, and M. Qian. 2014. Toll-like receptor-triggered calcium mobilization protects mice against bacterial infection through extracellular ATP release. *Infect. Immun.* 82: 5076–5085.
9. Akira, S., S. Uematsu, and O. Takeuchi. 2006. Pathogen recognition and innate immunity. *Cell* 124: 783–801.
10. Parkin, J., and B. Cohen. 2001. An overview of the immune system. *Lancet* 357: 1777–1789.
11. Chen, J., E. Baig, and E. N. Fish. 2004. Diversity and relatedness among the type I interferons. *J. Interferon Cytokine Res.* 24: 687–698.
12. Galligan, C. L., T. T. Murooka, R. Rahbar, E. Baig, B. Majchrzak-Kita, and E. N. Fish. 2006. Interferons and viruses: signaling for supremacy. *Immunol. Res.* 35: 27–40.
13. Schneider, W. M., M. D. Chevillotte, and C. M. Rice. 2014. Interferon-stimulated genes: a complex web of host defenses. *Annu. Rev. Immunol.* 32: 513–545.
14. Borden, E. C., G. C. Sen, G. Uze, R. H. Silverman, R. M. Ransohoff, G. R. Foster, and G. R. Stark. 2007. Interferons at age 50: past, current and future impact on biomedicine. *Nat. Rev. Drug Discov.* 6: 975–990.

15. Surprenant, A., and R. A. North. 2009. Signaling at purinergic P2X receptors. *Annu. Rev. Physiol.* 71: 333–359.
16. Lister, M. F., J. Sharkey, D. A. Sawatzky, J. P. Hodgkiss, D. J. Davidson, A. G. Rossi, and K. Finlayson. 2007. The role of the purinergic P2X7 receptor in inflammation. *J. Inflamm. (Lond.)* 4: 5.
17. Yang, D., Y. He, R. Muñoz-Planillo, Q. Liu, and G. Núñez. 2015. Caspase-11 requires the pannexin-1 channel and the purinergic P2X7 pore to mediate pyroptosis and endotoxic shock. *Immunity* 43: 923–932.
18. Idzko, M., D. Ferrari, and H. K. Eltzschig. 2014. Nucleotide signalling during inflammation. *Nature* 509: 310–317.
19. Solini, A., P. Chiozzi, A. Morelli, R. Fellin, and F. Di Virgilio. 1999. Human primary fibroblasts in vitro express a purinergic P2X7 receptor coupled to ion fluxes, microvesicle formation and IL-6 release. *J. Cell Sci.* 112: 297–305.
20. Ferrari, D., C. Pizzirani, E. Adinolfi, R. M. Lemoli, A. Curti, M. Idzko, E. Panther, and F. Di Virgilio. 2006. The P2X7 receptor: a key player in IL-1 processing and release. *J. Immunol.* 176: 3877–3883.
21. Qin, J., G. Zhang, X. Zhang, B. Tan, Z. Lv, M. Liu, H. Ren, M. Qian, and B. Du. 2016. TLR-activated gap junction channels protect mice against bacterial infection through extracellular UDP release. *J. Immunol.* 196: 1790–1798.
22. Gavala, M. L., Z. A. Pfeiffer, and P. J. Bertics. 2008. The nucleotide receptor P2RX7 mediates ATP-induced CREB activation in human and murine monocytic cells. *J. Leukoc. Biol.* 84: 1159–1171.
23. Miller, C. M., N. R. Boulter, S. J. Fuller, A. M. Zakrzewski, M. P. Lees, B. M. Saunders, J. S. Wiley, and N. C. Smith. 2011. The role of the $P2X_7$ receptor in infectious diseases. *PLoS Pathog.* 7: e1002212.
24. Jiang, L. H. 2009. Inhibition of P2X(7) receptors by divalent cations: old action and new insight. *Eur. Biophys. J.* 38: 339–346.
25. Gudipaty, L., B. D. Humphreys, G. Buell, and G. R. Dubyak. 2001. Regulation of P2X(7) nucleotide receptor function in human monocytes by extracellular ions and receptor density. *Am. J. Physiol. Cell Physiol.* 280: C943–C953.
26. Ruffell, D., F. Mourkioti, A. Gambardella, P. Kirstetter, R. G. Lopez, N. Rosenthal, and C. Nerlov. 2009. A CREB-C/EBPbeta cascade induces M2 macrophage-specific gene expression and promotes muscle injury repair. *Proc. Natl. Acad. Sci. USA* 106: 17475–17480.
27. Humphreys, B. D., J. Rice, S. B. Kertesy, and G. R. Dubyak. 2000. Stress-activated protein kinase/JNK activation and apoptotic induction by the macrophage P2X7 nucleotide receptor. *J. Biol. Chem.* 275: 26792–26798.
28. Le Stunff, H., R. Auger, J. Kanellopoulos, and M. N. Raymond. 2004. The Pro-451 to Leu polymorphism within the C-terminal tail of P2X7 receptor impairs cell death but not phospholipase D activation in murine thymocytes. *J. Biol. Chem.* 279: 16918–16926.
29. Kanneganti, T. D., M. Lamkanfi, Y. G. Kim, G. Chen, J. H. Park, L. Franchi, P. Vandenabeele, and G. Núñez. 2007. Pannexin-1-mediated recognition of bacterial molecules activates the cryopyrin inflammasome independent of Toll-like receptor signaling. *Immunity* 26: 433–443.
30. Honda, K., H. Yanai, H. Negishi, M. Asagiri, M. Sato, T. Mizutani, N. Shimada, Y. Ohba, A. Takaoka, N. Yoshida, and T. Taniguchi. 2005. IRF-7 is the master regulator of type-I interferon-dependent immune responses. *Nature* 434: 772–777.
31. Balachandran, S., and A. A. Beg. 2011. Defining emerging roles for NF-κB in antivirus responses: revisiting the interferon-β enhanceosome paradigm. *PLoS Pathog.* 7: e1002165.
32. Gough, D. J., N. L. Messina, L. Hii, J. A. Gould, K. Sabapathy, A. P. Robertson, J. A. Trapani, D. E. Levy, P. J. Hertzog, C. J. Clarke, and R. W. Johnstone. 2010. Functional crosstalk between type I and II interferon through the regulated expression of STAT1. *PLoS Biol.* 8: e1000361.